DEVELOPMENT OF PROTEOMICS-BASED APPROACHES AND THERAPEUTICS TO IDENTIFY AND TARGET RET KINASE PROTEIN IN LETHAL PROSTATE CANCER

A THESIS SUBMITTED TO THE GRADUATION SCHOOL

OF THE UNIVERSITY OF MINNESOTA

BY

QUYNH CHAU DINH

IN PARTIAL FULFILLMENT OF THE REQUIREMENTS FOR THE DEGREE

OF MASTER OF SCIENCE

Advisor: Justin M. Drake, Ph.D.

December 2024

Acknowledgements

I would like to thank Dr. Justin Drake for being a great mentor in this scientific journey. I am deeply thankful that I have the opportunity to work in Dr. Drake's lab and have as much exposure to doing research as possible. I also want to express my gratitude to all my lab mates for their great help and assistance – many thanks to Dr. Songyi Bae, Sachi Bhalchandra Tengse, Saasha Vinoo, Dr. Ali Arafa, Dr. Megan Ludwig, Gabby Larson, Alec Horrman, and Dr. Zoi Sychev. I am very grateful for Dr. Songyi Bae's guidance and mentorship since the first day I joined this lab. And I am grateful for Gabby in conducting and designing experiments for one of my most important projects in this lab. I also want to send my special thanks to Sachi for being such a great friend and lab buddy!

I feel extremely motivated with all of Drake lab's collaborators – Dr. Justin Hwang, Dr. Daniel Harki, Dr. Martin M. Matzuk – and want to say thank you for all of the guidance and amazing collaborations. It was truly a one-of-a-kind science experience.

I am incredibly grateful for my thesis committee, Dr. Scott Dehm and Dr. Julie Ostrander for their thoughtful guidance and for their insights on my thesis and project development.

I want to express my gratitude to my parents, who always support me in pursuing knowledge and always remind me to take care of myself. They have been the biggest motivators in my life. Also, I am grateful for my boyfriend's assistance and mental support in this journey.

ABSTRACT

Neuroendocrine prostate cancer (NEPC) is a subtype of metastatic castration resistant prostate cancer (mCRPC). It arises as a resistance mechanism to second generation androgen deprivation therapy (ADT). Platinum-based chemotherapy is often indicated as first-line treatment, however, they only provided minimal benefit. Therefore, there is a need to identify new therapeutic targets for NEPC and stratify patients for personalized medicine. Our lab has found that RET protein could serve as a potential therapeutic target for NEPC. RET is a receptor tyrosine kinase, which is often translocated or mutated in lung cancer and in different subsets of neuroendocrine tumors. We found that RET mRNA levels were elevated in mCRPC patients with a NEPC phenotype and in NEPC patient-derived xenografts (PDXs) compared to adenocarcinoma samples. There are two new FDA-approved RET inhibitors, and these therapies show efficacy in cancers such as papillary thyroid cancer and non-small cell lung cancer with RET fusions. We would like to expand the scope of these studies to prostate cancer and identify mCRPC patients that will potentially benefit from RET inhibition therapy. To do that, I propose using targeted mass spectrometry to identify patients with high abundance of RET protein in circulating tumor cells (CTCs). I hypothesize that liquid biopsy-based detection of RET kinase protein will aid in the stratification of patients with mCRPC. I have identified 10 candidate RET peptides that perform well on the mass spectrometer. Future studies will include evaluating these peptides for their ability to detect endogenous RET protein in pre-clinical and clinical samples. To identify new RET inhibitors, I also evaluated the effects of novel RET inhibitors on RET activity and its downstream signaling in NEPC cell line models. Novel RET inhibitors were able to reduce the activity of RET, AKT, and ERK phosphorylation. In addition, a mechanistic study also revealed the role of ASCL1 on RET in prostate cancer. These results are aimed to build the needed tools that support the hypothesis that RET is important for the survival of NEPC tumors and assessing RET expression will aid in the treatment of mCRPC/NEPC patients.

TABLES OF CONTENTS

LIST OF FIGURES

LIST OF TABLES

CHAPTER I: DEVELOPMENT OF RET PROTEOMIC-BASED ASSAY

I.1. Introduction

I.1.1. Prostate Cancer and disease progression

Prostate cancer is the most commonly diagnosed type of cancer among American men. It also ranks second in the leading cause of cancer death among American men. For every 41 men, one will die of prostate cancer (American Cancer Society, 2024). The development of prostate cancer initially relies on the activity of androgen receptor (AR) signaling. AR produces prostate-specific antigen (PSA) and promotes tumor growth (Hou et al., 2021). At diagnosis, patients are presented with localized or in some cases, metastatic prostate cancer. When patients have localized disease, radiation or localized androgen deprivation therapy (ADT) is used to treat these patients. Unfortunately, a subset of patients will present with metastatic prostate cancer at diagnosis. When patients are presented with treatment naïve metastatic prostate cancer, first generation ADT is indicated as the treatment in combination with hormonal therapy or docetaxel. In both cases, some patients will continue to develop resistance against first generation ADT and the tumors become castration resistant (Beltran et al., 2014, 2016). In metastatic castration resistant prostate cancer (mCRPC), patients are treated with second generation ADT, such as abiraterone, darolutamide, apalutamide, or enzalutamide initially followed by chemotherapy, PARP inhibitors, and/or PSMA-targeting therapy once hormonal therapy becomes futile (Bluemn et al., 2017; Miller et al., 2021). Eventually, and unfortunately, these men will die from prostate cancer (Fig. 1).

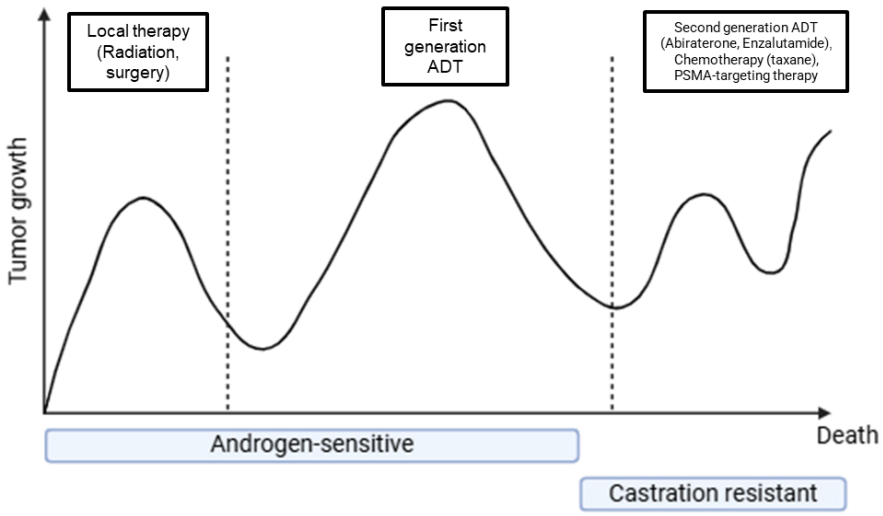

Figure 1. Prostate cancer disease progression.

Adapted from Miller et al., Prostate cancer, 2021. (Created in Biorender)

I.1.2. Overview of Neuroendocrine Prostate Cancer (NEPC) and RET kinase protein

Neuroendocrine prostate cancer (NEPC) is a subset of mCRPC. It arises from resistance to second generation ADT in which AR expression is significantly reduced concomitant with the expression of neural gene markers. NEPC tumors are highly aggressive with neuroendocrine morphological features, loss of *RB1* gene and mutation of the *TP53* gene (Beltran et al., 2014, 2016). The loss of AR in NEPC makes ADT less effective because cells can proliferate independently of AR signaling. Some neuroendocrine features that are overexpressed in NEPC include chromogranin A, ASCL1 and Rearranged during Transfection (RET) kinase (Fig. 2) (Tsai et al., 2017; Drake et al., 2013). RET is a receptor tyrosine kinase that requires a co-receptor (GFRα1/GFRα2) and secreted ligand (GDNF, ARTN, NRTN, or PSPN) to be activated (Ban et al., 2017). The mutation or translocation of RET is often found in lung cancer, thyroid cancer and some neuroendocrine cancers (Kouvaraki et al., 2005; Kato et al., 2017). Research in our lab found that there was an increase in RET mRNA and RET S969 phosphorylation in NEPC patient derived xenografts (PDX) compared to adenocarcinoma samples (Sychev et al., 2024). When RET was silenced in NCI-H660 cells,

cell growth was reduced (VanDeusen et al., 2020). These studies indicate that RET protein is overexpressed in NEPC tumors and is important for cell growth and survival.

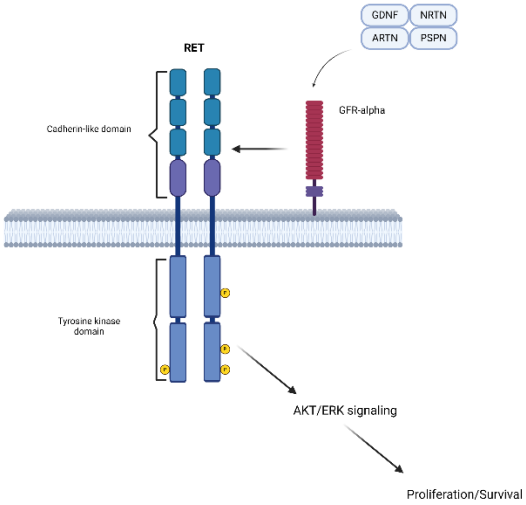

Figure 2. RET protein structure and overview of its signaling pathway.

RET was illustrated as a dimer with three regions: extracellular domain (containing cadherine-like domain), intracellular domain (containing tyrosine kinase domain) and transmembrane domain. The co-receptor GFR-alpha was illustrated in red. There are four ligands that bind to the co-receptor in this figure: GDFN, NTRN, ARTN, PSPN. RET downstream signaling pathway is AKT/ERK signaling. (Created in Biorender)

I.1.3. The Advantage of targeted Mass Spectrometry

Targeted mass spectrometry provides a data-independent acquisition method to detect peptides with high sensitivity and quantification (Picotti et al., 2009). Targeted proteomics can quantify protein levels that are associated with different diseases and different stages of a disease (Gillette and Carr, 2013). Therefore, it can provide specific diagnosis and aid in the process of subtype classification, thus enabling the prediction for targeted therapies in different subtypes of patients (Gillette and Carr, 2013; Ellis et al,

2013; De Marchi et al., 2016a, 2016b). Moreover, targeted mass spectrometry does not require the use of antibody, which is often costly and time consuming to develop. Targeted mass spectrometry can provide protein quantitation assays that are precise and reproducible for a big variety of biomarkers.

Targeted mass spectrometry has huge advantages for its high sensitivity and specificity. In targeted proteomics, the target is predetermined. There are two filtering steps, MS1 and MS2, which help to increase the signal-to-noise ratio. Sensitivity will also be enhanced because the mass spectrometer will need to scan and analyze only the peptides of interest, so it does not need to spend time analyzing other peptide ions (van Bentum and Selbach, 2021) (Fig. 3).

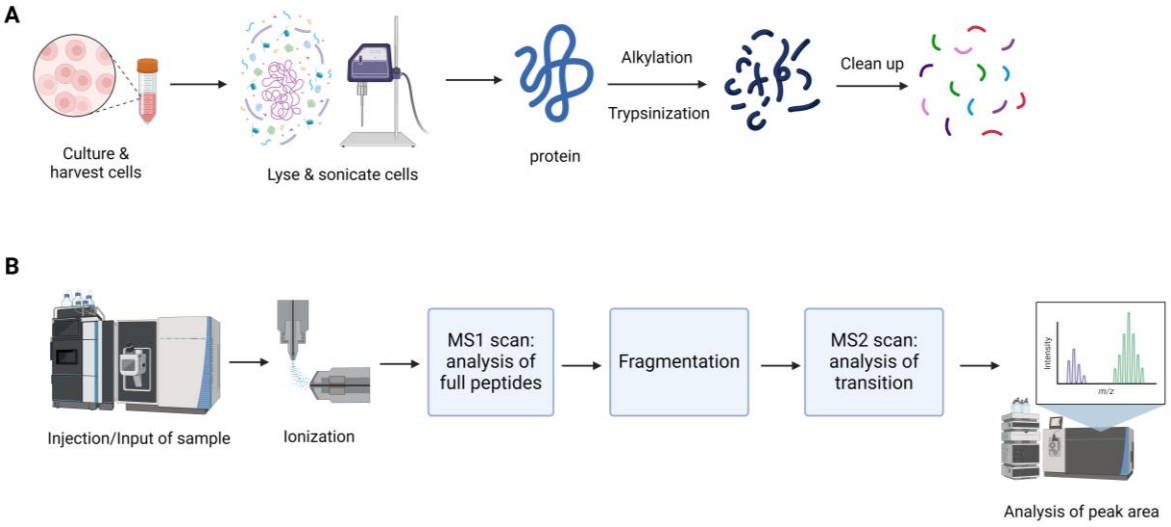

Figure 3. Targeted Mass Spectrometry workflow.

Cell preparation for mass spectrometry analysis. Cells are harvested, lysed, sonicated, alkylated and trypsinized to extract peptides. Then, peptides are cleaned up to de-salt for mass spectrometry column. The amount of peptides to be injected onto mass spectrometry is determined by peptide assay (Fluorometric or Colorimetric Peptide assay). B, Peptide samples are injected onto mass spectrometer. Samples are ionized, converted to gas phase and accelerated. Ions are scanned as full-length peptides in first spectra MS1. Ions are selectively fragmented prior to the second spectra MS2. MS2 scan analyzes the transition of the ions. Lastly, ions are analyzed for peak area. (Created in BioRender)

I.2. Methods & Materials

I.2.1. Mass spectrometry sample preparation & running

Extracellular recombinant human RET protein (aa 1 – 635) was purchased from Sino Biosciences. Intracellular recombinant human RET protein (aa 658 – 1114) was purchased from Abcam. The protein was reconstituted in HPLC grade water (Thermo Fisher) at the concentration of 1μg/uL. To digest the protein, 1-2μg of protein was incubated with 2% SDS with phosphatase (Thermo Fisher 78428) and protease (Millipore Sigma) inhibitors added, cleaned up via SP3 column, incubated with Trypsin and LysC with ratio of 1:50 and 1:200 respectively, cleaned up with C18 stage tip and freeze dried. The samples were reconstituted in 0.1% formic acid, 2% acetonitrile prior to running on the Lumos Orbitrap. Running method was built via XCalibur.

RET-specific AQUA peptides were ordered from Thermo Fisher. The peptides were diluted in HPLC grade water (Thermo Fisher) to make stock of 5pmol/μL and they were stored at -20°C. Two peptides GSIVGGHEPGEPR and DAPEEVPSFR were prepared in matrix of 293T cells. The matrix was digested following the procedure described in the previous paragraph. Then, 1fmol of each peptide was injected onto the mass spectrometer in each run. Running method was built via XCalibur.

I.2.2. Mass spectrometry data analysis

Shotgun mass spectrometry data was analyzed using MaxQuant, R Studio and Microsoft Excel Spreadsheet. MaxQuant was used to analyze technical replicates from sample runs and it generated the data based on canonical and isoform sequences that were obtained from Uniprot human reference proteome database (2016). R Studio was used to clean up and organize sequences of peptides according to their protein and gene names. Microsoft Excel was used to generate heatmaps of the peptides in each run.

Targeted mass spectrometry data was analyzed using Skyline-Daily (Skyline). Setting of transition is in the process of optimization.

I.3. Results

I.3.1. Top 10 Candidate RET Peptides

We have found out top 10 candidate RET peptides from recombinant human RET protein, 5 peptides from intracellular domain and 5 peptides from extracellular domain (Table 1). These peptides were checked for mis-cleavage sites, peptide length, peptide solubility, peptide composition. The criteria to choose a peptide included: the peptide must be unique to the protein of interest, the peptide matches with the spectral library, the peptide is 6 – 10 amino acids in length, the peptide does not start with a glutamine, the peptide does not contain methionine and glycosylation site, the peptide does not contain mis-cleavage site (Adapted from Zoi Sychev, Ph.D.). The peptides that did not meet the requirements will be eliminated. The peptides were blasted using NCBI protein database to ensure they were unique to human RET protein. Then, heatmaps were generated using Excel Spreadsheet to evaluate which peptides were the most frequent and consistent in 4 biological and 8 technical replicates.

RET peptides from extracellular domain	RET peptides from intracellular domain
1. GSIVGGHEPGEPR (588-600)	6. AGYTTVAVK (750-758)
2. LGQHLYGTYR (68-77)	7. ALPSTWIENK (1051-1060)
3. DAPEEVPSFR (58-67)	8. TLGEGEFGK (729-737)
4. SLDHSSWEK (100-108)	9. NILVAEGR (879-886)
5. VFDADVVPASGELVR (298-312)	10. VGPGYLGSGGSR (822-833)

Table 1. Top 10 candidate RET peptides.

The peptides were generated from extracellular and intracellular domains of the RET protein. Their amino acids are described in parentheses.

I.3.2. Evaluating the performance of 2 RET peptides GSIVGGHEPGEPR and DAPEEVPSFR on Lumos Orbitrap

The light peptide of GSIVGGHEPGEPR eluted after 21.8 minutes. All three transitions co-eluted at the same time (Fig. 4A). The light peptide of DAPEEVPSFR eluted after 38.7 minutes. All three transitions co-eluted at the same time (Fig. 4B). The peaks of these peptides were clearly distinct from the background. These data proved that the two peptides can fly well on the mass spectrometer and can be detected by the mass spectrometer. Also, they do not co-elute at the same time, which means that they have the potential to be used altogether for the detection of endogenous RET protein in cells, PDXs and clinical samples. We will further evaluate the performance of the remaining candidate RET peptides along with the optimization of collision energy, sensitivity and resolution, so we can determine the best peptides that are consistent and stable and allow for the detection of endogenous RET protein in NEPC cell lines and PDX samples at sufficient sensitivity and resolution, aiming at 100 attomoles (1amol = 10^{-18} moles) or 1μg of protein.

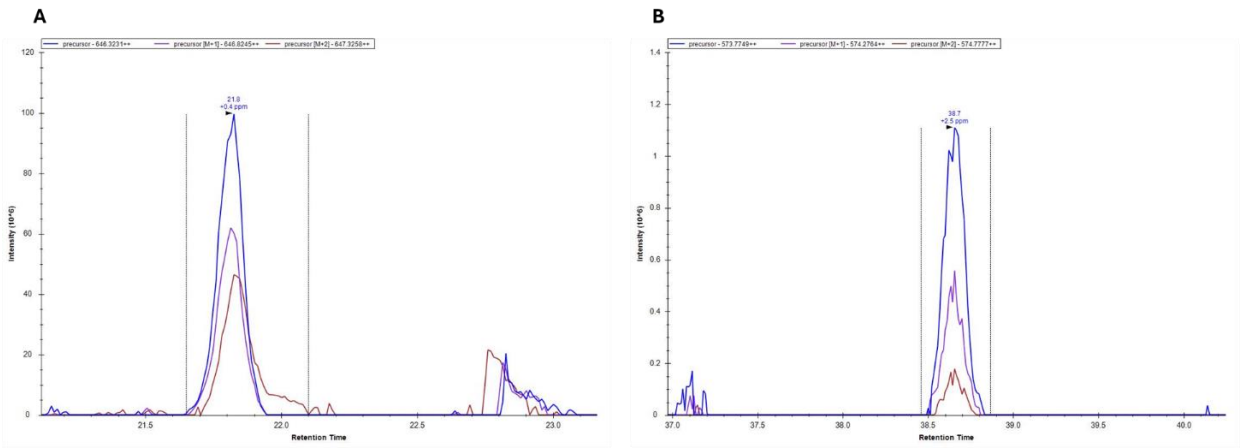

Figure 4. RET peptides GSIVGGHEPGEPR (A) and DAPEEVPSFR (B).

1fmol of each RET peptide GSIVGGHEPGEPR and DAPEEVPSFR was prepared in 1μg of 293T matrix and injected onto the Lumos Orbitrap (n=2), and their chromatograms were analyzed using Skyline-Daily. Transition setting was set for all matching scans with no indication for collision energy and optimization library. Figure 4 showed technical replicate 1.

CHAPTER II: ASSESSING THE EFFECTS AND EFFICACY OF NOVEL RET INHIBITORS

II.1. Introduction

II.1.1. Overview of FDA-approved RET Inhibitors

The FDA approved two RET-specific inhibitors as well as a few multikinase inhibitors that also inhibit RET activity. The two RET-specific inhibitors showed promise in treating RET-positive and RET-altered cancers. The two inhibitors that specifically target RET protein are selpercatinib and pralsetinib.

Pralsetinib (BLU-667) is a small-molecule RET inhibitor, and it targets wild type RET protein and RET alterations. In the clinical trial ARROW, patients who had RET-positive solid tumors received the treatment with pralsetinib. These patients had RET fusion non-small cell lung cancer (NSCLC), medullary thyroid cancer (MTC) and some other types of tumors. In patients who had received platinum chemotherapy before, the response rate was 61% (53 out of 87 patients). The median progression-free survival of this group was 17.1 months. In patients who did not receive platinum chemotherapy, the response rate was 70% (19 out of 27 patients). The median progression-free survival of the latter group was 11.6 months. And the overall survival of pralsetinib in this clinical trial was 13.6 months. There was no reported case of death that was due to the use of pralsetinib (Gainor et al., 2021; Gouda and Subbiah, 2023).

Selpercatinib is a small-molecule RET inhibitor and it exerts its effect through the ATP binding mechanism. Selpercatinib targets a variety of RET fusions and RET mutations. In the clinical trial LIBERTTO-001, patients who had metastatic solid tumor with RET-positive NSCLC received treatment with selpercatinib. In patients who had previously received platinum chemotherapy, the response rate was 61%, and 18 out of 247 patients had complete response. The median-free survival of this group was 24.9 months. In patients without platinum chemotherapy, the response rate was 84%, and 4 out of 69 patients had complete response. The median-free survival of this group was 22 months. Based on these results,

selpercatinib was approved by the FDA for treating patients with metastatic RET fusion NSCLC (Drilon et al., 2022; Gainor et al., 2021).

Overall, pralsetinib and selpercatinib proved their selectivity in targeting wild type RET protein and RET-positive fusion and mutation tumors. The former studies showed their efficacy in reducing tumor growth in NSCLC or MTC. However, mutations also arose as a resistance mechanism against selpercatinib and pralsetibnib. G810C/S and Y806C/N were identified as RET mutants in treatment with selpercatinib. In the cell lines that acquired G810C/S, V804M and M918T mutations, the autophosphorylation of RET was not inhibited when treated with selpercatinib (Subbiah et al., 2021). The cells that had these mutations will have 18- to 334-fold higher IC_{50} values in both pralsetinib and selpercatinib (Subbiah et al., 2021). We would like to expand the scope of the studies on RET-specific inhibitors into prostate cancer, where RET is understudied. In addition, we aim to identify novel RET inhibitors that can target RET specifically and can overcome the challenges of drug resistance like RET fusions and mutations.

II.2. Methods & Materials

II.2.1. Cell culturing

NCI-H660 (H660) was cultured in SCM media made from Advanced DMEM/F12 media (Gibco) with 10% fetal bovine serum (FBS) (Sigma Aldrich), 1X B27 Supplement (Gibco), 10ng/mL EGF (PeproTech), 10ng/mL bFGF (PeproTech), 1% penicillin-streptomycin (Life Technologies), and 1X Glutamax (Life Technologies). The cells were passaged every 5 days at the ratio of 1:3. 293T cells were cultured in DMEM with 10% FBS (Sigma Aldrich), 1% Glutamax (Life Technologies) and 10% penicillin-streptomycin (Life Technologies). RET-overexpressed 293T cells were cultured in DMEM with 10% FBS (Sigma Aldrich) and 1% Glutamax (Life Technologies). 293T cells were passaged every 5 days at the ratio of 1:16. All the cells were incubated in a humidified incubator at 37°C and 5% CO_2.

II.2.2. Generating stable overexpression cell lines

Retroviral particles were made by transfecting 293T cells with 20µg RET-wild type plasmid, 15µg pVSV-g, 15µg pMD-gag and calcium chloride. 293T cells were transduced with the retrovirus using 10µg/mL polybrene. After 48 hours of transduction, 293T stable cells were selected with 1µg/mL puromycin.

II.2.3. RET Inhibitors

RET inhibitors were screened by Dr. Martin M Matzuk from Baylor College of Medicine. The method of screening was affinity selections with unknown tagged proteins to pulldown high-affinity binders (Fig. 5). RET was identified as high affinity off target from selected compound. We received 8 RET inhibitors: CDD-2535, CDD-2612, CDD-2807, CDD-2598, CDD-2649, CDD-2211, CDD-2764 in 10mM DMSO stocks and CDD-2762 in 200µM DMSO stock.

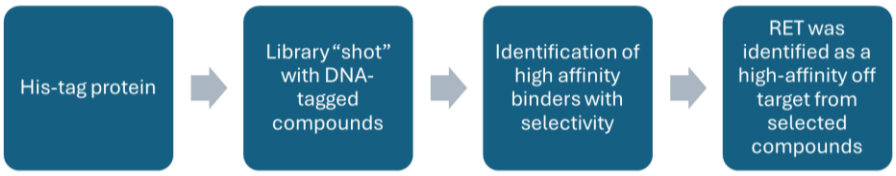

Figure 5. RET inhibitor screening process.

Shared by Dr. Martin M. Matzuk and Dr. Daniel Harki.

II.2.4. Cell proliferation assay and IC50 measurement

Five thousand H660 cells were seeded in each well (n=3) of a 96-well plate and incubated with RET inhibitors for 4 days. The concentrations of these inhibitors included: 30µM, 10µM, 3.33µM, 1.11µM, 370nM, 123.35nM, 41.12nM, 0nM and control for 10mM stock inhibitors; 1µM, 333.33nM, 111.11nM, 37.04nM, 12.35nM, 4.12nM, 0nM and control for 200 µM stock. Positive control was BLU-667. The

concentrations of BLU-667 were: 100μM, 30μM, 10μM, 3.33μM, 1.11μM, 370nM, 123.35nM, 41.12nM, 0nM and control. The drug was diluted in DMSO.

After 4 days, reagent WST (Takara) was added to H660 cells using protocol from manufacturer. Cell proliferation was measured on a TECAN plate reader with absorbance wavelength of 450nm and reference wavelength of 650nm.

IC50 measurement was conducted using GraphPad Prism v.10. Values were generated from one WST assay with 3 replicates for each condition.

II.2.5. Western Blotting

H660 and 293T cells were lysed with 2% SDS with phosphatase (Thermo Fisher 78428) and protease (Millipore Sigma) inhibitors added. The protein concentration was determined by Micro BCA Protein Assay Kit (Thermo Fisher). 25μg of protein was loaded on 4–20% protein gel (Mini-PROTEAN® TGX Stain-Free™, BioRad), transferred to PVDF membrane, and blocked with 5% BSA in 1xTBS for 30 minutes at room temperature. The membranes were incubated with primary antibody with the ratio of 1:800 at 4°C overnight. The primary antibodies included: Total RET (E1N8X Cell Signaling Technology), total RET (3223 Cell Signaling Technology), total AKT (4691S Cell Signaling Technology), total ERK (9102 Cell Signaling Technology, ASCL1 D-7 (Santa Cruz sc-374104), phospho-RET Y905 (3221 Cell Signaling Technology), phospho-RET Y1062 (PA5-104769 Introvigen), phosphor-AKT S473 (9271S Cell Signaling Technology), phosphor-ERK ½ (9102 Cell Signaling Technology), TetR (TET02 Abcam), β-actin (Santa Cruz sc47778). Then, the membranes were washed with 1xTBST, incubated with Licor-IR conjugated secondary antibody with the ratio of 1:5000 for one hour at room temperature. The membranes were washed again with 1xTBST and imaged on ChemiDoc Imaging System. ImageJ Fiji was used to assess the effects of RET inhibitors on RET signaling and RET downstream signaling.

II.3. Results

II.3.1. Novel RET Inhibitors are more potent than current FDA-approved RET Inhibitors & IC_{50} values

I performed the cell proliferation assay on NCI-H660 cells and analyzed their IC_{50} values. The top 4 RET inhibitors were CDD-2535, CDD-2612, CDD-2598, CDD-2807 with IC_{50} values of 4.27μM, 2.45μM, 3.46μM and 1.73μM respectively (Fig. 6). These inhibitors were more potent than positive control BLU-667, whose IC_{50} was 19μM (Fig. 6). IC_{50} values of CDD-2649 and CDD-2762 cannot be determined. Since the inhibitor CDD-2649 was dissolved in low stock concentration, it was not possible to have a sufficient range of concentrations to create an IC_{50} curve. IC_{50} values of CDD-2211 and CDD-2764 were not consistent throughout different replicates (Fig. 6, Table 2). Their IC_{50} values were between 13μM and 23μM, which was close or higher than the IC_{50} value of BLU-667. I decided to move forward with the top 4 RET inhibitors.

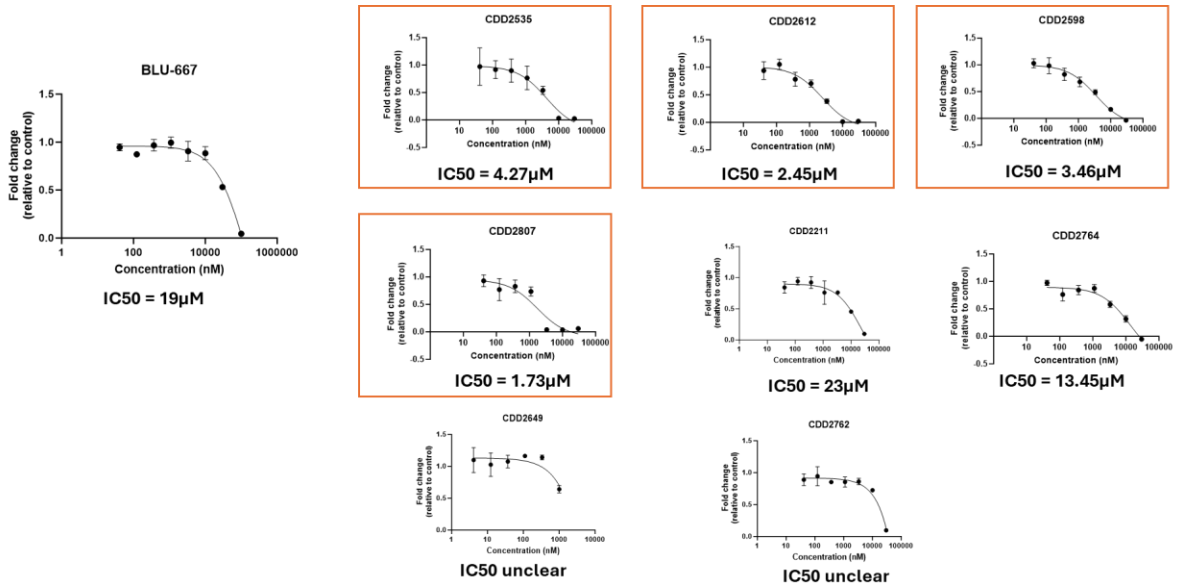

Figure 6. IC_{50} curves of 8 RET inhibitors.

The top four RET inhibitors are highlighted in red boxes, including CDD-2535, CDD-2612, CDD-2598, CDD-2807. Mean value and standard deviation were generated with 4th trial with 3 technical replicates. Created in GraphPad Prism v.10.

RET inhibitor	Trial 1	Trial 2
CDD-2535	2.824 μM	4.273μM
CDD-2598	4.335μM	3.466μM
CDD-2612	1.504μM	2.458μM
CDD-2807	6.194μM	1.731μM
CDD-2649	291.6nM	TBD
CDD-2211	13.596μM	~23μM
CDD-2764	4.098μM	13.454μM
CDD-2762	4.580μM	TBD

Table 2. IC50 values of 8 RET inhibitors.

The top four RET inhibitors are highlighted in bold font, including CDD-2535, CDD-2612, CDD-2598, CDD-2807. Data was generated in GraphPad Prism v.10.

II.3.2. Novel RET Inhibitors reduce RET activity and its downstream signaling

We assessed the effects and efficacy of top 4 RET inhibitors (CDD-2535, CDD-2598, CDD-2807, CDD-2612) in RET-overexpressed 293T cells. Total RET wild type, phospho-RET Y905 and phosphor-RET Y1062 were overexpressed in RET-293T cells (Fig. 7). The two inhibitors CDD-2535 and CDD-2598 performed better at reducing RET activity, AKT and ERK activity. The effects of downregulation of downstream signaling can be observed from 100nM and higher concentration (Fig. 8, Fig. 9). This pattern cannot be observed in Fig. 9D for the inhibitor CDD-2598 due to derivation from data quantification. The effects of downregulating RET, AKT, and ERK activity of CDD-2612 and CDD-2598 can be observed at 1μM (Fig. 8, Fig. 9).

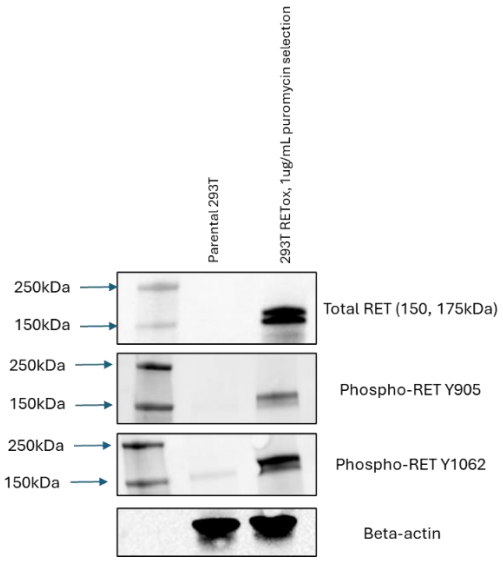

Figure 7. Overexpression of RET wild type in 293T cells.

Cells were transduced with 20µg RET-wild type plasmid and selected with 1µg/mL polybrene. Cells were lysed with 2% SDS (phosphatase and protease inhibitors added). 15µg of protein from cells was incubated with total RET (E1N8X Cell Signaling Technology), phospho-RET Y905 (3221 Cell Signaling Technology), phospho-RET Y1062 (PA5-104769 Introvigen) for one hour. The control was parental untransfected 293T cells and beta-actin (Santa Cuz sc47778) was used as a loading control.

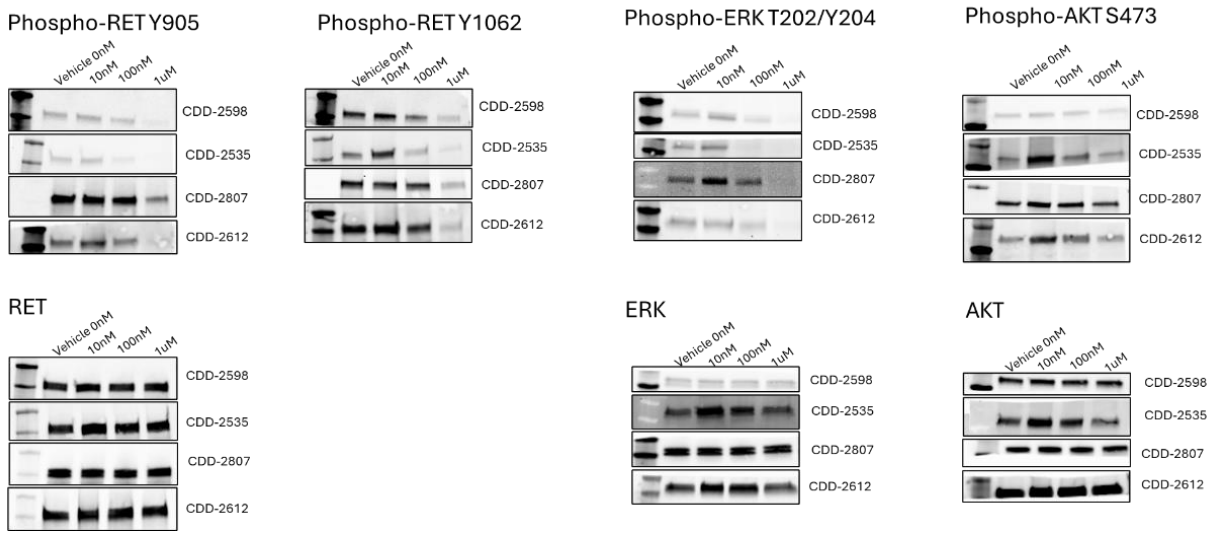

Figure 8. The effects of top 4 RET inhibitors on phospho-RET Y905, phospho-RET Y1062, phospho-AKT, and phospho-ERK.

Cells were lysed with 2% SDS (phosphatase and protease inhibitors added). 25µg of protein from cells was incubated with total RET (E1N8X Cell Signaling Technology), total AKT (4691S Cell Signaling Technology), total ERK (9102 Cell Signaling Technology), phospho-RET Y905 (3221 Cell Signaling Technology), phospho-RET Y1062 (PA5-104769 Introvigen), phospho-AKT S473 (9271S Cell Signaling Technology), phosphor-ERK ½ (9102 Cell Signaling Technology), β-actin (Santa Cruz sc47778).

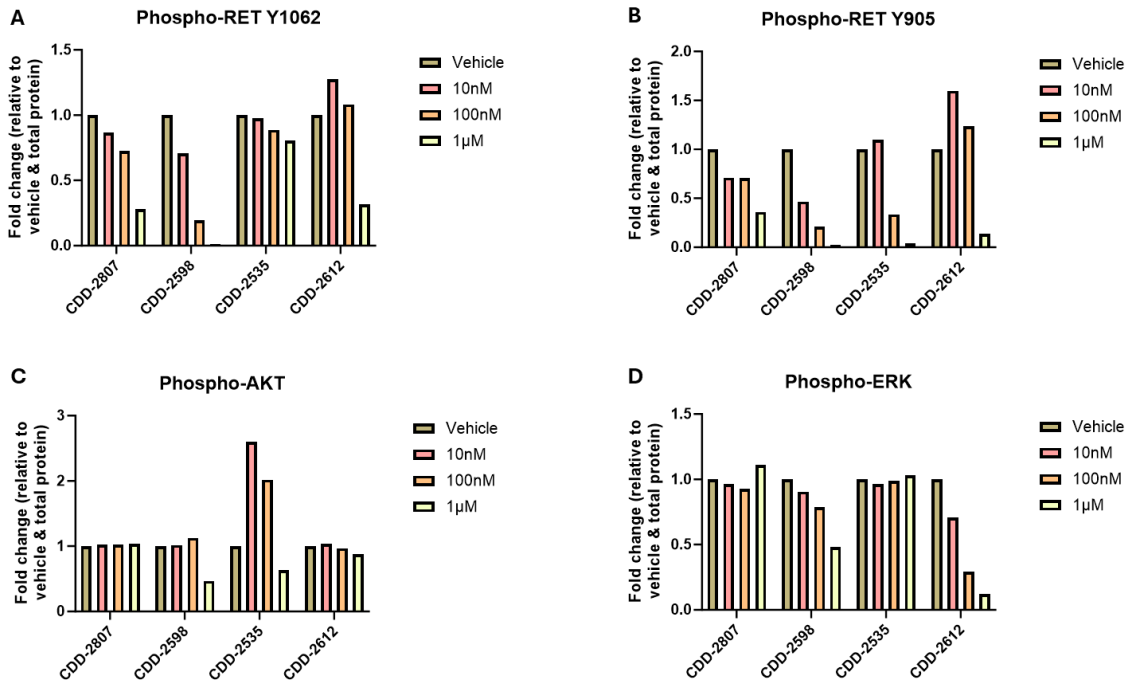

Figure 9. Data quantification of the effects of top 4 RET inhibitors on phospho-RET Y905, phospho-RET Y1062, phospho-AKT, and phospho-ERK.

Results were normalized with total protein and vehicle. Values were generated as area and intensity of Western Blot bands by ImageJ Fiji. Graphs were created in GraphPad Prism v.10.

CHAPTER III: DISCUSSION OF CHAPTER I & CHAPTER II

We have identified 10 candidate peptides for detecting endogenous RET protein using RET recombinant protein. It proved that full length recombinant protein can be used to design peptides to be used in targeted mass spectrometry experiments. By using recombinant protein, we can ensure that the set of peptides will not co-elute at the same time and these peptides can fly well on the mass spectrometer. We also examined the sensitivity of both the Quantiva and Lumos Orbitrap mass spectrometers. Traditionally, the Quantiva mass spectrometer is often used for targeted mass spectrometry and the method is Multiple Reaction Monitoring (MRM). Our lab made the decision to switch to the Lumos Orbitrap because the method of the Lumos Orbitrap was Parallel Reaction Monitoring (PRM), which is more sensitive than MRM. This is an advantage because we would like to move forward in this project with the analysis of circulating tumor cells (CTCs) in patient samples, and we estimated that we will only collect 100-200 cells per patient. The sensitivity of the method should reach single digit attomole based on 10,000 RET molecules per cell. Future studies will focus on choosing the suitable and best-performing peptides to detect endogenous RET protein in pre-clinical and clinical samples.

Furthermore, we found that novel RET inhibitors are more potent than FDA-approved RET inhibitor BLU-667. These inhibitors can effectively kill NEPC cells NCI-H660 in the range of 1μM and 10μM. They also showed their effects in downregulating downstream signaling of RET that promotes cell growth and cell proliferation like Erk and Akt. BLU-667 was designed to target some common RET fusions like RET-KIF5B and RET-CCDC6 and constitutively active RET mutations like RET C634W and RET M918T (Subbiah et al., 2018). However, it was reported that BLU-667 had little impact on the Akt signaling pathway (Subbiah et al., 2018). These novel RET inhibitors showed the potential to improve the treatment of RET-positive cancer patients. Future studies will include analyzing inhibition effects and spectrum of these RET inhibitors. These studies will confirm RET as a key biomarker in mCRPC/NEPC patients and promote treatment using RET targeting drugs and combination therapies in mCRPC/NEPC patients.

CHAPTER IV: DEVELOPMENT OF TOOLS TO ASSESS RET AND ASCL1 FUNCTION AND SIGNALING PATHWAY IN NEPC

IV.1. Introduction

IV.1.1. Overview of ASCL1

ASCL1, achaete-scute family bHLH transcription factor 1, is a regulator that participates in the process of neuronal and neuroendocrine differentiation. In a study in small cell lung cancer (SCLC), ASCL1 inactivation led to the halt of neuroendocrine tumor development (Rudin et al., 2019). Also, our lab found that ASCL1 is highly expressed in neuroendocrine-positive tumors compared to adenocarcinoma samples (Sychev et al., 2024). Targeting ASCL1 and defining the signaling network consisting of RET and ASCL1 in prostate cancer can further profile the characteristics of NEPC and develop targeting therapies.

IV.2. Methods & Materials

IV.2.1. Generating stable knockdown cell lines

Lentiviral particles were made by transfecting 293T cells with 20ug pLKO.1 shScr, pLKO.1 shRET4, pLKO.1 shRET5, pLKO.1 shASCL1-1, pLKO.1 shASCL1-4 plasmids, 13µg pMDL, 5µg pRev, 7µg pVSVg and calcium chloride. H660 cells were transduced with the lentivirus using 10µg/mL polybrene (Sigma Aldrich). After 48 hours of transduction, H660 cells were selected with 0.5µg/mL puromycin.

Lentiviral particles were made by transfecting 293T cells with 20ug Tet-pLKO.1 shRET4, Tet-pLKO.1 shRET5, Tet-pLKO.1 shASCL1-1, Tet-pLKO.1 shASCL1-4 and Tet-pLKO.1 shScr plasmids, 13µg pMDL, 5µg pRev, 7µg pVSVg and calcium chloride. 293T cells were transduced with the lentivirus using 10µg/mL polybrene. After 48 hours of transduction, 293T cells were selected with 1µg/mL puromycin.

Lentiviral particles were made by transfecting 293T cells with 20µg Tet-pLKO.1 shRET4, Tet-pLKO.1 shRET5, Tet-pLKO.1 shASCL1-1, Tet-pLKO.1 shASCL1-4 and Tet-pLKO.1 shScr plasmids, 13µg

pMDL, 5μg pRev, 7μg pVSVg and calcium chloride. After 48 hours of transduction, H660 cells were selected with 0.2μg/mL and 0.5μg/mL puromycin.

IV.2.2. Doxycycline induction in inducible cell lines

Doxycycline was made in 1mg/mL stock and filtered through 0.22μm syringe filter. H660 cells were separated into single cells, seeded to 96-well plate with cell density of 5000 cells/well. After 72 hours, the cells were incubated with WST reagent (Takara) and measured on TECAN plate reader. GraphPad Prism was used to create a kill curve for doxycycline in H660 cells.

H660 cells that were transfected with Tet-pLKO.1 shRET5, Tet-pLKO.1 shASCL1-1, Tet-pLKO shASCL1-4 plasmids were incubated with 2000ng/mL and 5000ng/mL of doxycycline for 4 days. Western Blotting (Section II.2.5) was performed to evaluate the effect of doxycycline on turning on the silencing gene of RET and ASCL1.

IV.3. Results

IV.3.1. Doxycycline effects on H660 cells

Doxycycline has no profound toxicity on H660 cells. Toxicity of doxycycline was negligible in the presence of 2000ng/mL to 10ng/mL doxycycline. (Fig. 10). I concluded that doxycycline was safe for H660 cells and can move forward to treat doxycycline in inducible H660 cell lines.

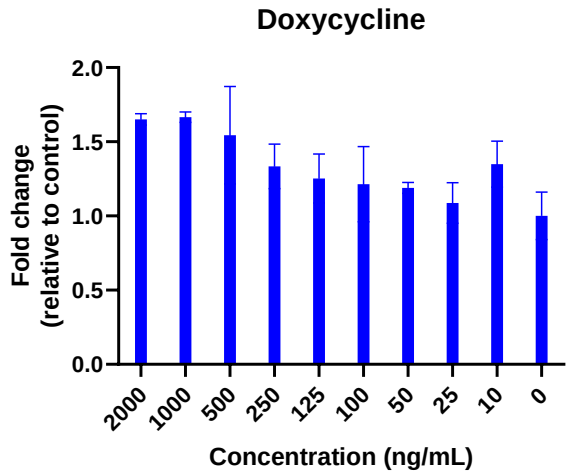

Figure 10. Doxycycline kill curve of NCI-H660 cells.

H660 cells were incubated with 9 concentrations of doxycycline, starting at 2000ng/mL, serially diluted at the ratio of 1:2 for 72 hours. Control was H660 cells in SCM. Cells were incubated with WST reagent (Takara) at the ratio of 1:10 and measured on M100 TECAN plate reader with absorbance wavelength of 450nm and reference wavelength of 650nm. Results were normalized with control condition, n=3. Created in GraphPad Prism v.10.

IV.3.2. Partial knockdown of ASCL1 was observed using inducible model

We performed transducing inducible plasmids in 293T cells to see whether the plasmids can be packaged into the cells. Except Tet-pLKO.1 shRET4, all of the plasmids can be transduced into cells when blotted against TetR protein (Fig. 11). I moved forward with transducing Tet-pLKO.1 shScr, Tet-pLKO.1 shRET5, Tet-pLKO.1 shASCL1-1, Tet-pLKO.1 shASCL1-4 into H660 cells.

In H660 cells, ASCL1 was partially knockdowned in the presence of 2000ng/mL and 5000ng/mL doxycycline compared to control Tet-pLKO.1 shScr (Fig .12). However, RET was not knockdowned in either of the two conditions described above (Fig. 12).

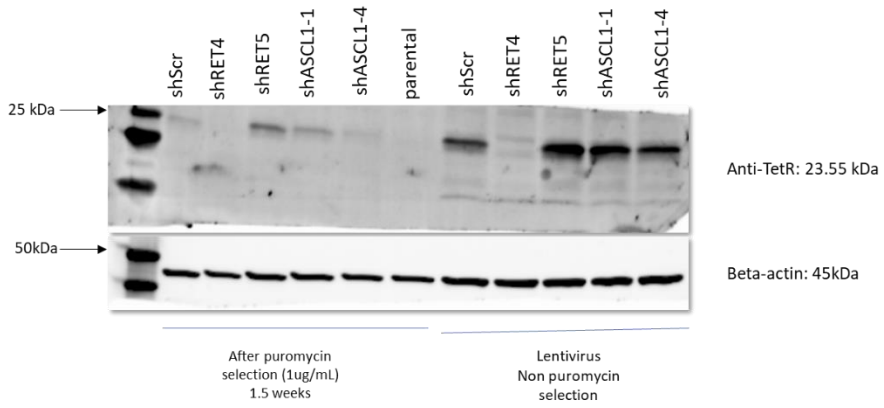

Figure 11. Inducible knockdown of RET and ASCL1 using Tet-pLKO.1 shRNA RET and ASCL1 plasmids in 293T cells.

293T cells were transduced with 20ug Tet-pLKO.1 shRET4, Tet-pLKO.1 shRET5, Tet-pLKO.1 shASCL1-1, Tet-pLKO.1 shASCL1-4, Tet-pLKO.1 shScr plasmids, and selected with 1µg/mL puromycin. 15µg of protein from cells was incubated with TetR (TET02 Abcam). Beta-actin (Santa Cuz sc47778) was used as a loading control.

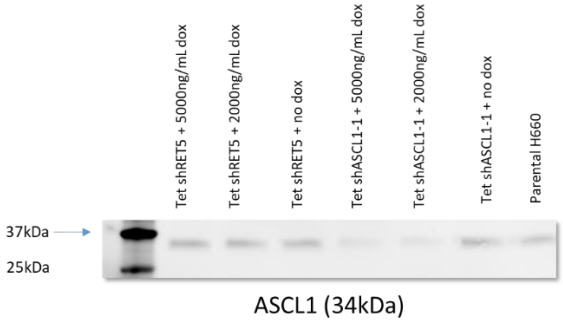

Figure 12. Doxycycline induced knockdown effects of shRET5, shASCL1-1, shASCL1-4 in NCI-H660 cells.

H660 cells were transduced with 20ug Tet-pLKO.1 shRET4, Tet-pLKO.1 shRET5, Tet-pLKO.1 shASCL1-1, Tet-pLKO.1 shASCL1-4, Tet-pLKO.1 shScr plasmids, and selected with 0.2µg/mL puromycin. 15µg of protein from cells was incubated with total ASCL1 (Santa Cruz sc-374104).

In a different experiment, when treated with doxycycline, Tet-pLKO.1 shRET5 expression was reduced compared to control Tet-pLKO.1 shScr (Fig. 13) However, the effects of knockdown in Tet-pLKO.1 shASLC1-1 and Tet-pLKO.1 shASCL1-4 were not clear compared to parental H660 cells treated with doxycycline (Fig. 13).

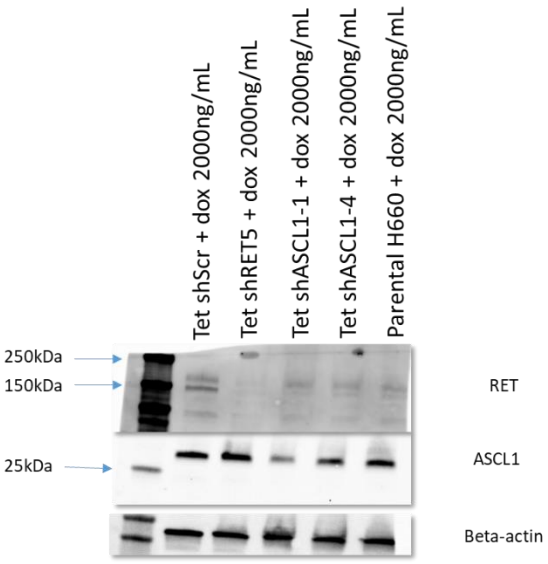

Figure 13. Doxycycline effects of Tet-pLKO.1 shRET4, Tet-pLKO.1 shRET5, Tet-pLKO.1 shASCL1-1, Tet-pLKO.1 shASCL1-4 in NCI-H660 cells.

H660 cells were transduced with 20ug Tet-pLKO.1 shRET4, Tet-pLKO.1 shRET5, Tet-pLKO.1 shASCL1-1, Tet-pLKO.1 shASCL1-4, Tet-pLKO.1 shScr plasmids, and selected with 0.2µg/mL puromycin. 15µg of protein from cells was incubated with total RET (3223 Cell Signaling Technology), total ASCL1 (Santa Cruz sc-374104). Beta-actin (Santa Cuz sc47778) was used as a loading control.

IV.4. Discussion

ASCL1 is a regulator of neuronal of lineage plastic and contributes to the neuroendocrine differentiation (Nouruzi et al., 2022). One study showed that targeting ASCL1 can reverse the neuroendocrine lineage. In addition, RET is upregulated in neuroendocrine tumors and can be a therapeutic

target in prostate cancer. In lung adenocarcinoma, the microarray-based gene expression profile showed higher level of expression of RET protein in ASCL1-positive tumors compared with ASCL1-negative tumors. In the same study, the knockdown experiment using ASCL1 shRNA in adenocarcinoma lung cells indicated that ASCL1 is a potential upstream regulator of the RET protein (Kosasri et al., 2014). We are in the process of defining the transcriptional relationship between ASCL1 and RET in prostate cancer. Research in our lab also showed the strong correlation of RET expression with ASCL1 and also higher RET expression in NEPC tumors. These data suggest that there is a direct regulatory mechanism between RET and ASCL1, and also that this pathway is related to the development of neuroendocrine tumors. We want to further prove this hypothesis with more models, and currently we are developing overexpression and knockdown model to assess the regulatory relationship between ASCL1 and RET. Knocking down RET and ASCL1 directly using shRNA is detrimental to NEPC cells as ASCL1 and RET is important for the cell growth. To overcome this challenge, we switched to using the inducible knockdown model Tet-shRNA. The results from this experiment confirmed that NEPC cells can be transduced with Tet-shRNA plasmids. Also, the treatment with doxycycline can partially turn on the silencing gene of ASCL1. Future studies will include optimizing the doxycycline concentration and cell treatment conditions to have a complete knockdown of all plasmids in NEPC cells and determining the direction of ASCL1 and RET regulatory pathway. We believe that studying the relationship between ASCL1 and RET proteins can help us further understand the signaling pathway of NEPC and improve treatments for this disease by developing specific targeting therapies or combination therapies with the transcriptional factors that are involved in this pathway.

CHAPTER V: TROUBLESHOOTING AND ALTERNATIVE APPROACHES

V.1. Assessing the role of RET and ASCL1

Initially, we performed the knockdown experiment with RET and ASCL1 in H660 cells using pLKO.1 shRET4, pKLO.1 shRET5, pLKO.1 shASCL1-1 and pLKO.1 shASCL1-4 constructs. However, the cells could not survive after puromycin selection, meaning that they did not carry the knockdown plasmid. In one experiment, the effects of knocking down these genes cannot be observed (Fig. 14). Also, NCAM1 and BRN2 expression, ASCL1 downstream signaling, was not reduced (Fig. 14). There were 3 possible reasons for this: too high concentration of puromycin, low transduction efficiency in H660 cells, plasmids cannot be transduced. Since we have tested the transduction of these plasmids in 293T and H660, we tried to troubleshoot for the other two hypotheses. We reduced the concentration of puromycin from 0.5μg/mL to 0.2μg/mL in transduced H660 cells. And since the cells die after the transduction, and also RET and ASCL1 are important for cell growth, we switched to inducible models (Fig. 11, Fig. 12, Fig. 13). Currently, we are working on optimizing the doxycycline conditions to assess the knockdown effects and study the role of ASCL1 on RET.

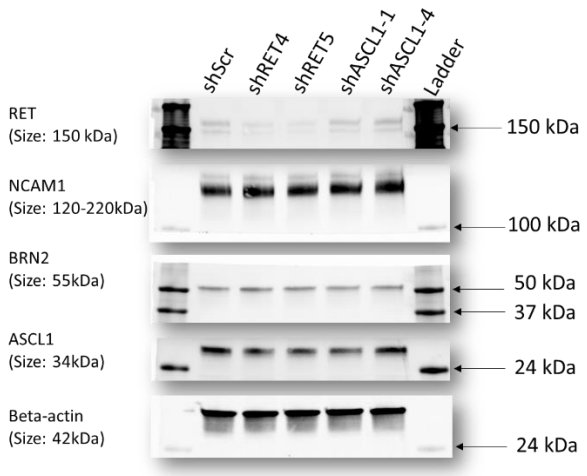

Figure 14. Knockdown RET and ASCL1 using shRNA plasmids in NCI-H660 cells.

H660 cells were transduced with 20ug shRET4, shRET5, shASCL1-1, shASCL1-4, shScr plasmids, and selected with 0.5μg/mL puromycin. 25μg of protein from cells was incubated with total RET (3223 Cell Signaling Technology), total ASCL1 (Santa Cruz sc-374104), NCAM 1 (Santa Cruz sc106), BRN2 (D2C1L Cell Signaling Technology). Beta-actin (Santa Cuz sc47778) was used as a loading control.

V.2. Testing available RET peptide for its ability to detect endogenous RET protein in H660 cells

Our lab has found one RET peptide in one of our PDX models. The peptide was RPAQAFPVSYSSSGAR. I ran this peptide on the mass spectrometer Lumos Orbitrap to confirm the co-elution of heavy and light peptide (Fig. 15). Light and heavy peptide was mixed in matrix of parental 293T, which did not express RET protein. However, we were not able to observe the detection of RET protein in H660 cells at low concentration using this peptide (Fig. 16). Later, I found that this peptide had a mis-cleavage site, thus, it can elevate the limit of detection (LOD) when detecting endogenous protein and it is not stable. Therefore, we decided not to move forward with this peptide and would use recombinant human RET protein to design RET peptides. (Table 1).

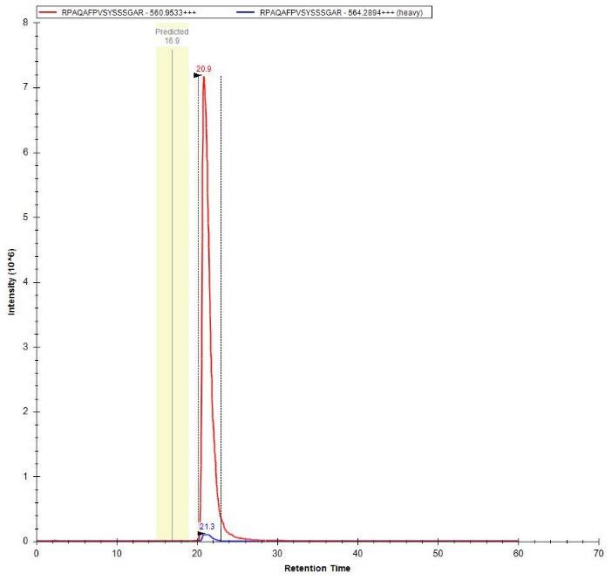

Figure 15. Co-elution of light and heavy peptides of RET peptide RPAQAFPVSYSSSGAR.

1000fmol of light peptide and 50fmol of heavy peptide were prepared in matrix of 293T cells and injected on the Quadrupole Quantiva. The run was unscheduled and scanned for all retention times.

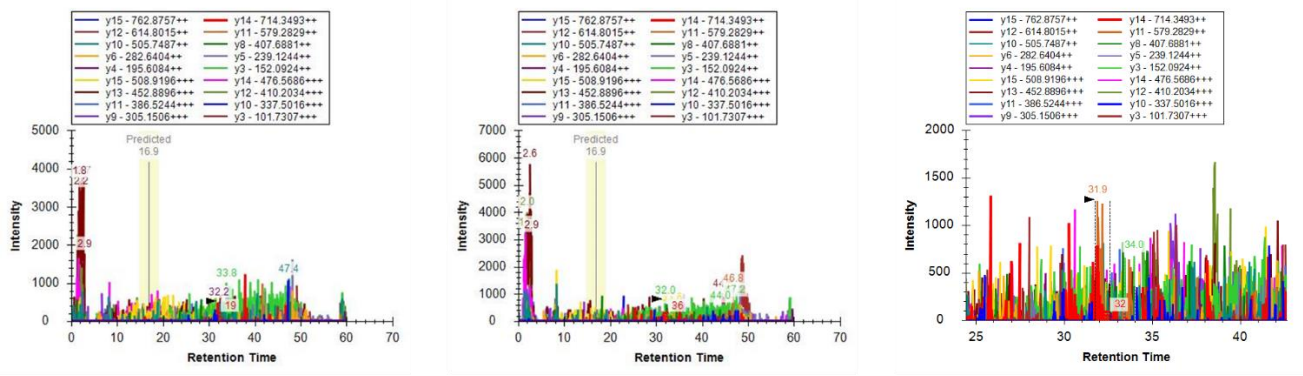

A. 2.5µg B. 5µg C. 10µg

Figure 16. Detection of endogenous RET protein in NCI-H660 cells using RET peptide RPAQAFPVSYSSSGAR.

2.5µg (A), 5µg (B), and 10µg (C) of digested H660 cells were prepared in matrix of 293T cells. These samples were run on Quadrupole Quantiva as unscheduled runs and scanned for all retention times.

CHAPTER VI: FUTURE DIRECTION

VI.1. Hypothesis 1: RET peptides are able to detect endogenous RET protein in cell lines and PDX models.

For future work, it will be important to validate the quality of the selected 10 RET peptides on the Lumos Orbitrap mass spectrometer. The method is reverse-phase liquid chromatography. The information of mass-to-charge and retention time of the peptide will be collected. There are five different experiments to be conducted to evaluate characteristics of a peptide: determining limit of detection, validating repeatability, evaluating specificity, evaluating stability, and validating the reproducible detection of endogenous RET in samples (CPTAC Assay Development Working Group).

a) To determine the limit of detection, a response curve will be created. The matrix used in these experiments is RET-negative cell lines and PDXs. First, matrix protein is lysed with 2% SDS, digested with LysC and Trypsin and cleaned up using C18 stage tip. Serially diluted concentrations of light peptides will be mixed with constant concentrations of the heavy peptide in the matrix. The standard includes a blank, which is just heavy peptide in matrix, and at least 6 different concentration points. The standards will be injected onto the Lumos Orbitrap. After that, Skyline software will be used to generate a linear regression curve, determine the limit of detection (LOD), linearity, limit of quantification (LOQ) and lower limit of quantification (LLOQ).
b) To evaluate the repeatability of the peptides, three replicates of three different concentrations (low, medium and high concentration compared to LLOQ) are prepared with matrix, then spiked in with heavy peptide and run on the mass spectrometer. This experiment will be repeated for 4 days.
c) To evaluate the precision of the peptide, samples will be prepared in matrixes with different concentrations and injected onto the mass spectrometer as mentioned in experiment (a). The peak areas and intensity will be analyzed for standard deviation and variability.
d) To examine the specificity of the peptide, 3 to 6 biological replicates will be prepared in matrixes with different concentrations of heavy peptide plus one sample without heavy peptide. These

samples will be run in duplicate. The samples will be analyzed for standard deviation from the mean value as well as ion transition ratios.

e) To evaluate the stability of the peptide, different concentrations of light peptide and heavy peptide will be prepared in matrix and divided into 3 sets. In the first set, they are injected onto the mass spectrometer after 0 hour and 6 hours in duplicate. The second set will go through freezing at -80C and thawing process once and injected onto the mass spectrometer after 0 hour and 6 hours in duplicate. The third set will go through freezing at -80C and thawing process twice and injected onto the mass spectrometer after 0 hour and 6 hours in duplicate.

f) To validate the performance of the RET proteomic assay in NEPC cell lines and PDX models, two prostate cancer cell lines that express different levels of RET protein (NCI-H660, LASCPC-01) and two RET-negative cell lines (DU145, 22Rv1) are included in this experiment. Our lab will collaborate with Dr. Eva Corey at the University of Washington to acquire four RET-positive PDX models and four RET-negative PDX models to set the baseline levels of RET protein detection and generate a signal-to-noise ratio for our assay. Frozen PDX samples were shipped to our lab and have previously been lysed with urea buffer, cleaned up, and are ready to use. The cell line samples will be processed as follows: lysis of samples using 2% SDS, clean-up via SP3 protocol (Hughens et al., 2019), digestion with LysC and TPCK Trypsin, and clean-up and elution by C18 stage tips. Finally, all of the samples are spiked with heavy peptides, run in triplicate and measured for RET protein levels. These samples will also be processed the same way as other samples before being injected into the mass spectrometer. The experiment will be repeated 3 times.

VI.2. Hypothesis 2: Novel RET inhibitors can reduce RET expression and its downstream signaling in RET mutation models

To evaluate whether RET inhibitors can inhibit RET activation and its downstream signaling, RET mutation plasmids will be transduced into 293T cells. We have generated 3 mutation plasmids in the lab:

FU-RET C634W CRW, FU-RET M918T CRW and RET K758M. RET C624W and RET M918T are constitutively active and drug resistance mutations, and RET K758M is the kinase dead mutation. Total RET, phospho-RET Y905 and phospho-RET Y1062 were overexpressed when the mutations C634W and M918T were transfected to 293T cells (Fig. 17). Total RET protein expression was elevated in 293T cells that were transfected with K578M mutation (Fig. 17). These mutant cell lines will be treated with top 4 RET inhibitors for 4 hours, lysed with 2% SDS (phosphatase and protease inhibitor added), ran on on 4–20% protein gel (Mini-PROTEAN® TGX Stain-Free™, BioRad), transferred to PVDF membrane, and blocked with 5% BSA in 1xTBS for 30 minutes at room temperature. The membranes were incubated with primary antibody with the ratio of 1:800 at 4°C overnight. Then, the membranes were washed with 1xTBST, incubated with Licor-IR conjugated secondary antibody with the ratio of 1:5000 for one hour at room temperature. The membranes were washed again with 1xTBST and imaged on ChemiDoc Imaging System. ImageJ Fiji will be used to assess the effects of RET inhibitors on the mutant 293T cell lines.

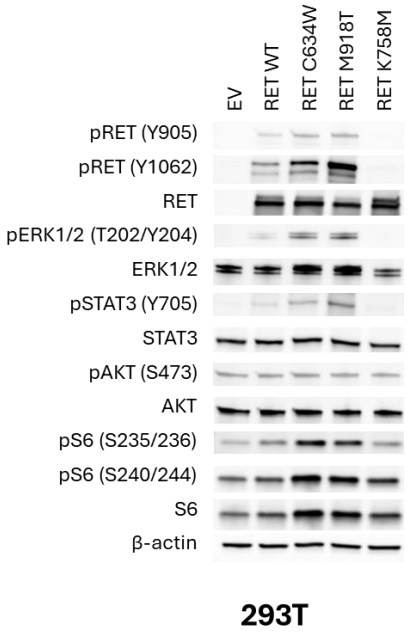

Figure 17. Overexpression of RET C634W, RET M918T and RET K758M in 293T cells.

Models were developed by postdoctoral researcher Dr. Songyi Bae.

REFERENCES

American Cancer Society. Key Statistics for Prostate Cancer | Prostate Cancer Facts. (2024). https://www.cancer.org/cancer/types/prostate-cancer/about/key-statistics.html

Ban, K., Feng, S., Shao, L., & Ittmann, M. (2017). RET signaling in prostate cancer. *Clinical Cancer Research*, *23(16)*, 4885–4896. https://doi.org/10.1158/1078-0432.ccr-17-0528

Beltran, H., Prandi, D., Mosquera, J. M., Benelli, M., Puca, L., Cyrta, J., Marotz, C., Giannopoulou, E., Chakravarthi, B. V. S. K., Varambally, S., Tomlins, S. A., Nanus, D. M., Tagawa, S. T., Van Allen, E. M., Elemento, O., Sboner, A., Garraway, L. A., Rubin, M. A., & Demichelis, F. (2016). Divergent clonal evolution of castration-resistant neuroendocrine prostate cancer. *Nature Medicine*, *22(3)*, 298–305. https://doi.org/10.1038/nm.4045

Beltran, H., Tomlins, S., Aparicio, A., Arora, V., Rickman, D., Ayala, G., Huang, J., True, L., Gleave, M. E., Soule, H., Logothetis, C., & Rubin, M. A. (2014). Aggressive variants of castration-resistant prostate cancer. *Clinical cancer research: an official journal of the American Association for Cancer Research*, *20(11)*, 2846–2850. https://doi.org/10.1158/1078-0432.CCR-13-3309

Bluemn, E. G., Coleman, I. M., Lucas, J. M., Coleman, R. T., Hernandez-Lopez, S., Tharakan, R., Bianchi-Frias, D., Dumpit, R. F., Kaipainen, A., Corella, A. N., Yang, Y. C., Nyquist, M. D., Mostaghel, E., Hsieh, A. C., Zhang, X., Corey, E., Brown, L. G., Nguyen, H. M., Pienta, K., Ittmann, M., Schweizer, M., True, L.D., Wise, D., Rennie, P.S., Vessella, R.L., Morrissey, C., Nelson, P.S. (2017). Androgen Receptor Pathway-Independent Prostate Cancer Is Sustained through FGF Signaling. *Cancer cell*, *32(4)*, 474–489.e6. https://doi.org/10.1016/j.ccell.2017.09.003

CPTAC Assay Development Working Group. Overview of assay characterization for the CPTAC assay portal. *In Assay Characterization Guidance Documents*. https://proteomics.cancer.gov/assay-portal/about/assay-characterization-guidance-documents

De Marchi, T., Kuhn, E., Dekker, L. J., Stingl, C., Braakman, R. B., Opdam, M., Linn, S. C., Sweep, F. C., Span, P. N., Luider, T. M., Foekens, J. A., Martens, J. W., Carr, S. A., & Umar, A. (2016). Targeted MS Assay Predicting Tamoxifen Resistance in Estrogen-Receptor-Positive Breast Cancer Tissues and Sera. *Journal of proteome research, 15(4)*, 1230–1242. https://doi.org/10.1021/acs.jproteome.5b01119

De Marchi, T., Liu, N. Q., Stingl, C., Timmermans, M. A., Smid, M., Look, M. P., Tjoa, M., Braakman, R. B., Opdam, M., Linn, S. C., Sweep, F. C., Span, P. N., Kliffen, M., Luider, T. M., Foekens, J. A., Martens, J. W., & Umar, A. (2016). 4-protein signature predicting tamoxifen treatment outcome in recurrent breast cancer. *Molecular oncology, 10(1)*, 24–39. https://doi.org/10.1016/j.molonc.2015.07.004

Drake, J. M., Graham, N. A., Lee, J. K., Stoyanova, T., Faltermeier, C. M., Sud, S., Titz, B., Huang, J., Pienta, K. J., Graeber, T. G., & Witte, O. N. (2013). Metastatic castration-resistant prostate cancer reveals intrapatient similarity and interpatient heterogeneity of therapeutic kinase targets. *Proceedings of the National Academy of Sciences of the United States of America, 110(49)*, E4762–E4769. https://doi.org/10.1073/pnas.1319948110

Drilon, A., Subbiah, V., Gautschi, O., Tomasini, P., de Braud, F., Solomon, B. J., Shao-Weng Tan, D., Alonso, G., Wolf, J., Park, K., Goto, K., Soldatenkova, V., Szymczak, S., Barker, S. S., Puri, T., Bence Lin, A., Loong, H., & Besse, B. (2022). Selpercatinib in Patients With RET Fusion-Positive Non-Small-Cell Lung Cancer: Updated Safety and Efficacy From the Registrational LIBRETTO-001 Phase I/II Trial. *Journal of clinical oncology: official journal of the American Society of Clinical Oncology, 41(2)*, 385–394. https://doi.org/10.1200/JCO.22.00393

Ellis, M. J., Gillette, M., Carr, S. A., Paulovich, A. G., Smith, R. D., Rodland, K. K., Townsend, R. R., Kinsinger, C., Mesri, M., Rodriguez, H., Liebler, D. C., & Clinical Proteomic Tumor Analysis

Consortium (CPTAC) (2013). Connecting genomic alterations to cancer biology with proteomics: the NCI Clinical Proteomic Tumor Analysis Consortium. *Cancer discovery, 3(10)*, 1108–1112. https://doi.org/10.1158/2159-8290.CD-13-0219

Gainor, J., Curigliano, G., Kim, DW., Lee, D., Besse, B., Baik, C., Doebele, R., Cassier, P., Lopes, G., Tan, D., Garralda, E., Paz-Ares, L., Cho, B., Gadgeel, S., Thomas, M., Liu, S., Taylor, M., Mansfield, A., Zhu, V., Clifford, C., Zhang, H., Palmer, M., Green, J., Turner, C., Subbiah, V. (2021). Pralsetinib for RET fusion-positive non-small-cell lung cancer (ARROW): a multi-cohort, open-label, phase 1/2 study. *The Lancet Oncology*, *Volume 22*, Issue 7, Pages 959-969, ISSN 1470-2045. https://doi.org/10.1016/S1470-2045(21)00247-3.

Gillette, M. A., & Carr, S. A. (2013). Quantitative analysis of peptides and proteins in biomedicine by targeted mass spectrometry. *Nature Methods, 10(1)*, 28–34. https://doi.org/10.1038/nmeth.2309

Gouda, A., & Subbiah, V. (2023). Precision oncology with selective RET inhibitor selpercatinib in RET-rearranged cancers. *Therapeutic advances in medical oncology, 15* 17588359231177015. https://doi.org/10.1177/17588359231177015

Hou, Z., Huang, S., Li, Z. (2021). Androgens in prostate cancer: A tale that never ends. *Cancer Letters*. Volume 516, Pages 1-12, ISSN 0304-3835. https://doi.org/10.1016/j.canlet.2021.04.010.

Hughes, C.S., Moggridge, S., Müller, T., Sorensen, P. H., Morin, G. B., Krijgsveld, J. (2019). Single-pot, solid-phase-enhanced sample preparation for proteomics experiments. *Nature Protocol 14*, 68–85. https://doi.org/10.1038/s41596-018-0082-x

Kato, S., Subbiah, V., Marchlik, E., Elkin, S. K., Carter, J. L., & Kurzrock, R. (2017). *RET* Aberrations in Diverse Cancers: Next-Generation Sequencing of 4,871 Patients. *Clinical cancer research: an official journal of the American Association for Cancer Research, 23(8)*, 1988–1997. https://doi.org/10.1158/1078-0432.CCR-16-1679

Kosari, F., Ida, C., Aubry, MC., Yang, L., Kovtun, I., Klein, J., Yi, L., Erdogan, S., Tomaszek, S., Murphy, S., Bolette, L., Kolbert, C., Yang, P., Wigle, D., Vasmatzis, G. (2014). ASCL1 and RET expression defines a clinically relevant subgroup of lung adenocarcinoma characterized by neuroendocrine differentiation. *Oncogene 33*, 3776–3783. https://doi.org/10.1038/onc.2013.359

Kouvaraki, M. A., Shapiro, S. E., Perrier, N. D., Cote, G. J., Gagel, R. F., Hoff, A. O., Sherman, S. I., Lee, J. E., & Evans, D. B. (2005). RET Proto-Oncogene: A Review and Update of Genotype–Phenotype Correlations in Hereditary Medullary Thyroid Cancer and Associated Endocrine Tumors. *Thyroid*, *15(6)*, 531–544. https://doi.org/10.1089/thy.2005.15.531

Nouruzi, S., Ganguli, D., Tabrizian, N., Kobelev, M., Sivak, O., Namekawa, T., Thaper, D., Baca SC., Freedman, ML., Aguda, A., Davies. A., Zoubeidi, A. (2022). ASCL1 activates neuronal stem cell-like lineage programming through remodeling of the chromatin landscape in prostate cancer. *Nature Communication 13*, 2282. https://doi.org/10.1038/s41467-022-29963-5

Picotti, P., Bodenmiller, B., Mueller, L. N., Domon, B., & Aebersold, R. (2009). Full Dynamic Range Proteome Analysis of S. cerevisiae by Targeted Proteomics. *Cell*, *138(4)*, 795–806. https://doi.org/10.1016/j.cell.2009.05.051

Rudin, C. M., Poirier, J. T., Byers, L. A., Dive, C., Dowlati, A., George, J., Heymach, J. V., Johnson, J. E., Lehman, J. M., MacPherson, D., Massion, P. P., Minna, J. D., Oliver, T. G., Quaranta, V., Sage, J., Thomas, R. K., Vakoc, C. R., & Gazdar, A. F. (2019). Molecular subtypes of small cell lung cancer: a synthesis of human and mouse model data. *Nature reviews. Cancer*, *19(5)*, 289–297. https://doi.org/10.1038/s41568-019-0133-9

Subbiah, V., Gainor, J. F., Rahal, R., Brubaker, J. D., Kim, J. L., Maynard, M., Hu, W., Cao, Q., Sheets, M. P., Wilson, D., Wilson, K. J., DiPietro, L., Fleming, P., Palmer, M., Hu, M. I., Wirth, L., Brose, M. S., Ou, S. I., Taylor, M., Garralda, E., Miller, S., Wolf, B., Lengauer, C., Guzi, T, Evans, E.K.

(2018). Precision Targeted Therapy with BLU-667 for RET-Driven Cancers. *Cancer discovery*, *8(7)*, 836–849. https://doi.org/10.1158/2159-8290.CD-18-0338

Subbiah, V., Shen, T., Terzyan, S. S., Liu, X., Hu, X., Patel, K. P., Hu, M., Cabanillas, M., Behrang, A., Meric-Bernstam, F., Vo, P. T. T., Mooers, B. H. M., & Wu, J. (2021). Structural basis of acquired resistance to selpercatinib and pralsetinib mediated by non-gatekeeper RET mutations. *Annals of oncology: official journal of the European Society for Medical Oncology*, *32(2)*, 261–268. https://doi.org/10.1016/j.annonc.2020.10.599

Subbiah, V., Wolf, J., Konda, B., Kang, H., Spira, A., Weiss, J., Takeda, M., Ohe, Y., Khan, S., Ohashi, K., Soldatenkova, V., Szymczak, S., Sullivan, L., Wright, J., & Drilon, A. (2022). Tumour-agnostic efficacy and safety of selpercatinib in patients with RET fusion-positive solid tumours other than lung or thyroid tumours (LIBRETTO-001): a phase 1/2, open-label, basket trial. *The Lancet. Oncology*, *23(10)*, 1261–1273. https://doi.org/10.1016/S1470-2045(22)00541-1

Sychev, Z. E., Day, A., Bergom, H. E., Larson, G., Ali, A., Ludwig, M., Boytim, E., Coleman, I., Corey, E., Plymate, S. R., Nelson, P. S., Hwang, J. H., & Drake, J. M. (2024). Unraveling the Global Proteome and Phosphoproteome of Prostate Cancer Patient-Derived Xenografts. Molecular Cancer Research. *22(5)*, 452–464. https://doi.org/10.1158/1541-7786.MCR-23-0976

Tsai, H. K., Lehrer, J., Alshalalfa, M., Erho, N., Davicioni, E., & Lotan, T. L. (2017). Gene expression signatures of neuroendocrine prostate cancer and primary small cell prostatic carcinoma. *BMC Cancer*, *17(1)*. https://doi.org/10.1186/s12885-017-3729-z

van Bentum, M., & Selbach, M. (2021). An Introduction to Advanced Targeted Acquisition Methods. *Molecular & cellular proteomics 20*, 100165. https://doi.org/10.1016/j.mcpro.2021.100165

VanDeusen, H. R., Ramroop, J. R., Morel, K. L., Bae, S. Y., Sheahan, A. V., Sychev, Z., Lau, N. A., Cheng, L. C., Tan, V. M., Li, Z., Petersen, A., Lee, J. K., Park, J. W., Yang, R., Hwang, J. H.,

Coleman, I., Witte, O. N., Morrissey, C., Corey, E., & Nelson, P. S. (2020). Targeting RET Kinase in Neuroendocrine Prostate Cancer. *Molecular Cancer Research: MCR*, *18(8)*, 1176–1188. https://doi.org/10.1158/1541-7786.MCR-19-1245